GDCh

Research Articles

Angewandte
Chemie
International Edition
www.angewandte.org

VIP Reaction Networks *Very Important Paper*

Automated Generation of Microkinetics for Heterogeneously Catalyzed Reactions Considering Correlated Uncertainties**

Bjarne Kreitz,* Patrick Lott, Felix Studt, Andrew J. Medford, Olaf Deutschmann, and C. Franklin Goldsmith*

Abstract: The study presents an ab-initio based framework for the automated construction of microkinetic mechanisms considering correlated uncertainties in all energetic parameters and estimation routines. 2000 unique microkinetic models were generated within the uncertainty space of the BEEF-vdW functional for the oxidation reactions of representative exhaust gas emissions from stoichiometric combustion engines over Pt-(111) and compared to experiments through multiscale modeling. The ensemble of simulations stresses the importance of considering uncertainties. Within this set of first-principles-based models, it is possible to identify a microkinetic mechanism that agrees with experimental data. This mechanism can be traced back to a single exchange-correlation functional, and it suggests that Pt(111) could be the active site for the oxidation of light hydrocarbons. The study provides a universal framework for the automated construction of reaction mechanisms with correlated uncertainty quantification, enabling a DFT-constrained microkinetic model optimization for other heterogeneously catalyzed systems.

[*] Dr. B. Kreitz, Prof. Dr. C. F. Goldsmith
School of Engineering, Brown University
184 Hope Street, Providence, RI 02912 USA
E-mail: bjarne_kreitz@brown.edu
franklin_goldsmith@brown.edu

Dr. B. Kreitz, Dr. P. Lott, Prof. Dr. F. Studt,
Prof. Dr. O. Deutschmann
Institute for Chemical Technology and Polymer Chemistry, Karlsruhe Institute of Technology
Engesserstr. 20, 76128 Karlsruhe (Germany)

Prof. Dr. F. Studt
Institute of Catalysis Research and Technology, Karlsruhe Institute of Technology
76344 Eggenstein-Leopoldshafen (Germany)

Prof. Dr. A. J. Medford
School of Chemical and Biomolecular Engineering
Atlanta, GA 30318 (USA)

[**]A previous version of this manuscript has been deposited on a preprint server (https://doi.org/10.26434/chemrxiv-2023-hnb4 l).

Introduction

Microkinetic modeling of heterogeneously catalyzed reactions provides a tool to tailor catalytic materials and optimize reactor performance, but the elucidation of reaction pathways and parametrization of all steps and intermediates is a difficult and time-consuming process.[1] Reaction mechanisms are mainly studied by quantum mechanical (QM) calculations using density functional theory (DFT), since pathways can be investigated that are not accessible by experiments.[2,3] The main challenges in the mechanism construction are the computational cost of common DFT methods for the electronic structure calculations[4] as well as the considerable uncertainty in the DFT-derived properties. Fortunately, methods have become increasingly available that reduce the computational demands, either by replacing DFT with approximate scaling relations or by accelerating it with machine learning methods.[5] However, even with faster QM methods, the laborious task of predicting possible intermediates and pathways for a given catalytic system requires the researcher's chemical knowledge and intuition. Moreover, as the number of species increases or the species of interest get larger, a combinatorial explosion of potential pathways and intermediates occurs.[6,7] This complexity makes it easy for researchers to unintentionally miss kinetically relevant pathways. Ultimately, the omission of kinetically relevant steps in the mechanism can result in false predictions of the microkinetic model and, therefore, wrong conclusions about a process or catalyst.

Alternatively, exhaustive lists of all possible reactions can be generated from a set of initial species with generic bond-breaking recipes.[8,9] This approach runs the risk of including a swath of reactions that are kinetically irrelevant and, thus, increase the time to construct the mechanism and introduce stiffness. Additionally, the pathways are often selected based on the potential energy obtained at low coverages and 0 K, and they are not based on the actual rates at operating conditions, which can lead to misidentification of relevant pathways. Software can be employed to overcome this hurdle, which automatically constructs complex microkinetic models without any bias, considering all possible pathways at the operating conditions of the process. The Reaction Mechanism Generator (RMG)[10,11] is such an open-source tool that has been successfully employed for gas-phase chemistry[12,13] and heterogeneously catalyzed reactions.[14–18]

It has been shown in the literature that uncertainty in the energetic parameters has a tremendous effect on the

predicted activity, selectivity, and turnover frequency.[19–28] Further, considering correlations in the uncertainty of the energetic parameters is of paramount importance as it can lead to error cancellation[20] and affect the rate-determining steps.[19] Correlated uncertainties in the DFT energies within the GGA level of theory can be directly accessed from the semi-empirical BEEF-vdW functional.[29] Even though these uncertainties significantly affect the predictions, it is often assumed that the set of elementary reactions (the mechanism) is static, and only the energetic parameters (the microkinetics) are perturbed, even when screening catalytic materials across the periodic table.[20] In previous work, some of the authors used RMG to construct 5000 microkinetic models for the CO_2 methanation on Ni(111) by perturbing energetic parameters, assuming a simplified correlation according to linear scaling descriptors and BEP relations, resulting in drastic variations of the mechanisms.[16,17] Consequently, kinetically relevant species and pathways are heavily dependent on the energetic parameters. A more rigorous approach is to propagate the correlated uncertainty in all parameters during the bias-free automated mechanism generation procedure.

In this study, we significantly expand and improve our previous approach by sampling energetic parameters during the automated mechanism generation from the uncertainty space of the BEEF-vdW functional. Routines are implemented in RMG to estimate correlated uncertainties in energetic parameters for all previously unknown intermediates and elementary steps to explore all possible pathways. The method is applied to generate 2000 unique microkinetic models for the catalytic conversion of exhaust gas emission over a three-way catalyst (TWC) assuming a Pt(111) facet. The set of generated mechanisms is compared with experiments through multiscale modeling, which reveals a broad spread in the simulation results. In addition to new insights into the mechanism, the method is used as a tool for an ab-initio constrained optimization of the microkinetic model to achieve an excellent agreement with the experiment without explicit regression of parameters. Understanding the reaction mechanism and determining accurate microkinetics for this complex system is crucial to derive more compact and efficient TWC, e.g. for emission control in hybrid vehicles that use new dithering operation regimes.[30] The developed methodology is consistent with the correlated uncertainty in the energetic parameters in an unbiased mechanism construction and can serve as an approach that is universally applicable for other heterogeneously catalyzed reaction systems over different catalysts.

Results and Discussion

Mechanisms were automatically constructed using the open-source Reaction Mechanism Generator.[10,11,31,32] Figure 1 highlights the structure of RMG and illustrates the automated mechanism generation procedure.

The reader is referred to ref. [10,31] for details on RMG and to the Supporting Information for the salient features for this work; only a brief overview is provided here. All results and scripts can be found in ref. [33]. RMG explores all the possible gas-phase and surface chemistry according to the reaction templates by modifying the molecular graphs of the species with reaction templates, as determined by many reaction families. DFT-derived databases and estimation routines[34] are used to determine the thermophysical properties and kinetics of discovered intermediates and pathways, respectively. A rate-based algorithm decides if discovered species are deemed kinetically relevant,[35] i.e. their production rate exceeds a certain threshold in a reactor simulation at operating conditions, which interrupts the simulation and moves the species along with their reactions to the *core*; species that are formed by an elementary step but are kinetically insignificant are left in the *edge*. This procedure is repeated until a user-defined termination criterion is met during the simulation without discovering further kinetically relevant species, which terminates the mechanism expansion. The energetic parameters for the databases and reaction library were obtained from DFT calculations using the BEEF-vdW functional.[29] This semi-empirical functional was chosen as it provides accurate chemisorption energies[36] and the possibility to determine correlated uncertainties in the derived energies. After the self-consistent field calculation, it is possible to apply the Bayesian error estimate to perturb the parameters of the exchange-correlation functional and obtain an ensemble of 2000 non-self-consistent energies based on the uncertainty in the training of the functional. An ab-initio database of adsorbates on Pt-(111)[14,18] was extended within the present work to include 115 $C_xH_yO_z$* adsorbates containing up to 4 heavy atoms (see Supporting Information for QM details). We used the method of Blöndal et al.[14] to derive formation enthalpies from the DFT energies, which involves the usage of an adsorption reaction in combination with an isogyric reaction to determine the enthalpy of formation of the gas-phase precursor. The correlated uncertainty from the obtained ensemble of DFT-energies from the BEEF-vdW functional for the adsorbates in the database is directly propagated to the enthalpy of formation (see SI). Uncertainties in entropy and heat capacity are not considered; these uncertainties are assumed to be less significant, and they are harder to quantify.[37] An additional source of uncertainty that is not considered in this work is structural uncertainty due to the simplified representation of the complex Pt crystal morphology with a close-packed (111) facet. Pt(111) was chosen as it usually has the highest share of the exposed surface sites.[38] Thermophysical values of discovered gas-phase species are taken from available databases in RMG and they are considered to be exact within this study, as they are usually known with chemical (and sometimes sub kJ mol^{-1}) accuracy.[39] If a predicted species is not previously known (i.e. it is not in the database), RMG will estimate its thermophysical properties based on the gas-phase species and apply adsorption corrections to enthalpy, entropy, and heat capacity.[31,40] Adsorption corrections for the formation enthalpy are derived from the adsorbate database and corresponding gas-phase species. These corrections are organized in a tree-structured database that was overhauled within this work to provide improved estimates, especially
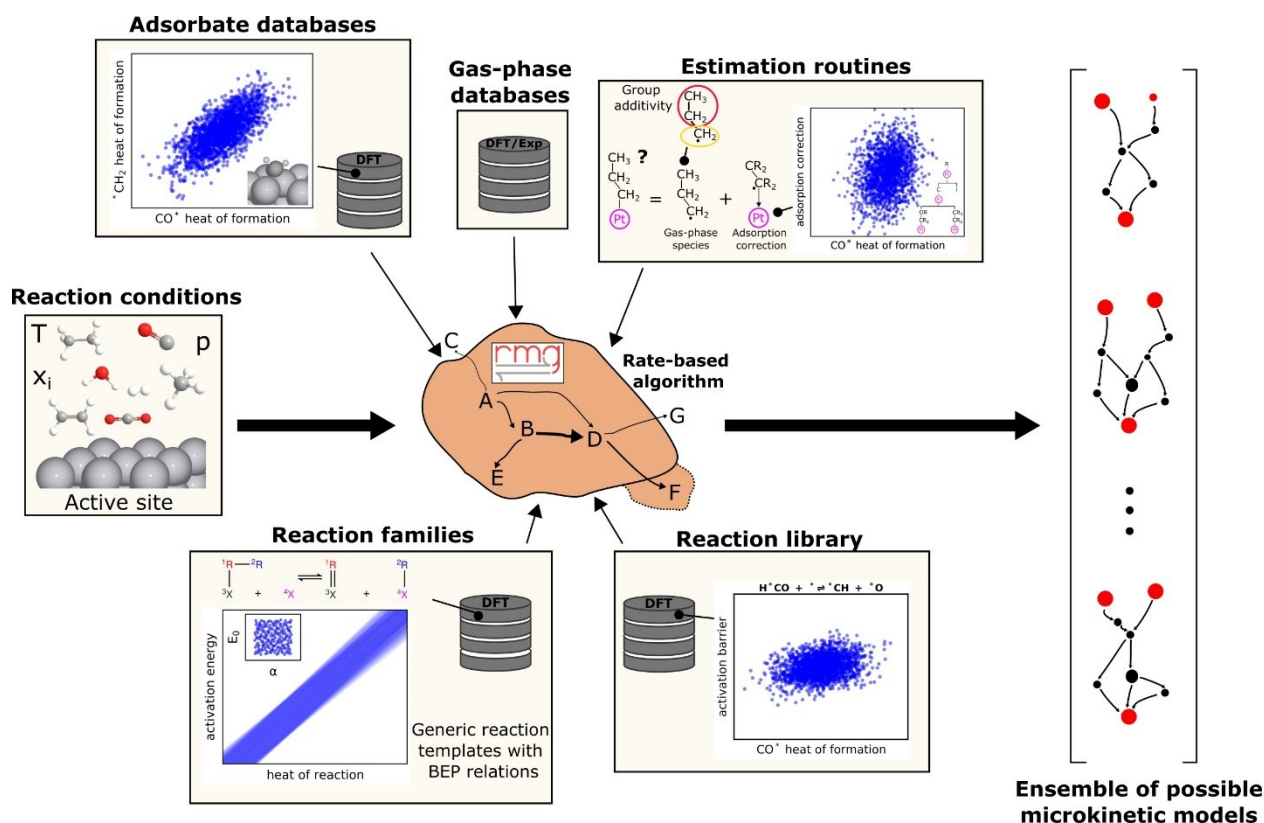
Figure 1. Schematic overview of the automated mechanism generation with RMG. All sources are highlighted where correlated uncertainty is introduced into the generation procedure. The adsorbates and reaction library use the results from the BEEF-vdW functional directly. Uncertainties in the adsorption correction are propagated from the adsorbate database. The uncertainty in the discovered reactions is based on BEP relations and consequently correlated with the reaction enthalpy.

for bidentate adsorbates (see Figure S2–S5). A reaction library with 27 elementary steps was constructed from QM calculations using the open-source saddle point search algorithm *SELLA*.[41] These reactions were identified to be the kinetically relevant pathways from a previous study conducted by the authors for this system.[18] Correlated uncertainties in the activation barrier of the elementary steps in the library are directly computed from the BEEF-vdW ensemble. Reaction kinetics of unknown elementary steps are estimated from Brønsted(Bell)-Evans-Polanyi (BEP) relations for generic reaction families similar to previous work.[16,18] BEP relations exploit the correlation of the reaction enthalpy with the activation barrier. Thus, all correlated changes in the enthalpy of formation of the intermediates are propagated to the activation barrier. Since BEP relations are only approximate, we added a quasi-random uncertainty via Sobol sequences to the intercept and slope of the BEP,[16] estimated from BEEF-vdW calculations[42] (see Figure S6).

RMG is set to generate mechanisms for the oxidation reactions of a representative exhaust gas mixture from stoichiometrically operated gasoline and natural gas engines[43] on a Pt(111) facet, based on light-out experiments with a 3 wt-% Pt/Al$_2$O$_3$ TWC monolith (see Figure 2a). The monolith was produced with a dip-coating procedure as detailed in ref. [18], resulting in an average Pt particle size of

1.8±0.2 nm (obtained from TEM measurements discussed in SI). Details on the catalyst synthesis, light-out experiments, and mechanism generation are provided in ref. [18] and in the SI. NO emissions were neglected in this study due to a lack of ab-initio data in RMG that prevents an exploration of the nitrogen chemistry, although it alters the conversion profiles of the emissions.[43] RMG is used to generate 2000 unique microkinetic models by drawing samples from the correlated high-dimensional uncertainty space;[16,17] a total of 277 parameters is simultaneously perturbed. With the additions and improvements to RMG, the software can estimate the energetic parameters of discovered elementary steps and intermediates along with their correlated uncertainties. Figure 2b shows RMG's estimated uncertainties for an unknown adsorbate (CH$_3$O*CO) and an unknown elementary reaction (dissociation of *CH$_2$CH$_3$). RMG does not find CH$_3$O*CO in the database of precompiled species, so it must estimate its thermophysical properties using the adsorption correction tree. The adsorbate in the gas phase is present in RMG's database, and the closest resemblance in the adsorption correction tree is *C(=O)R, where R is a generic rest. RMG estimates the formation enthalpy accurately with a deviation of 8 kJ mol^{-1} compared to the DFT value. Similarly, the correlated uncertainty distribution fits equally well with the non-self-consistent ensemble energies. The BEP relation for
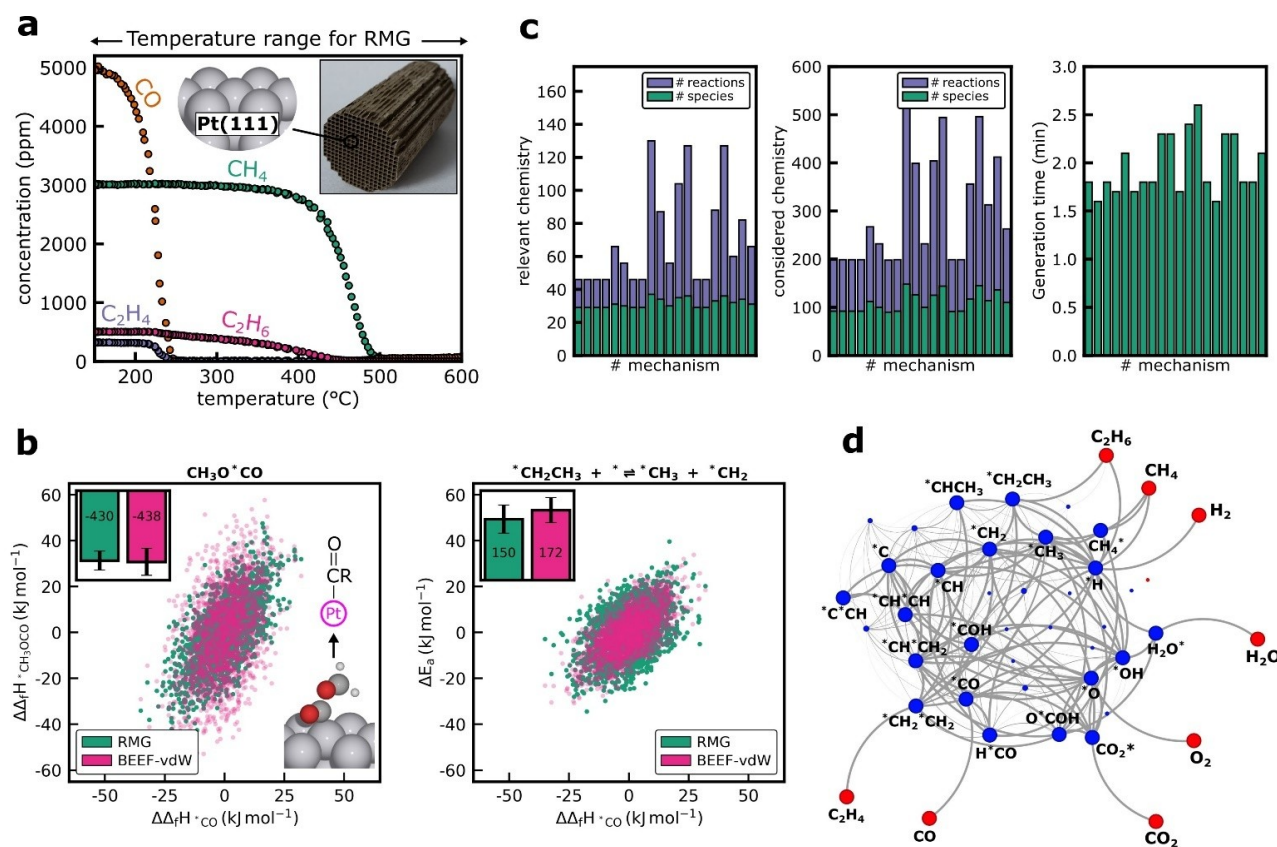
Figure 2. Experimental light-out curve for the oxidation of a representative emission mixture from stoichiometrically operated gasoline and natural gas engines over a 3 wt-% Pt/Al$_2$O$_3$ monolith.[18] b) Comparison of the correlated uncertainty estimate of RMG for an unknown adsorbates using the adsorption correction database and a reaction using the BEP relation for the breaking of C–C bonds of monodentate adsorbates with DFT results using the BEEF-vdW functional. The inset compares the average values in kJ mol^{-1} and the error bar shows the maximum deviation. *CO is arbitrarily used as a reference to illustrate the correlation. c) Metrics of the mechanism generation procedure for 20 randomly selected mechanisms. d) Reaction network from all 2000 individual microkinetic models. The size of the nodes highlights how often a species is discovered in a mechanism. The width of the edges illustrates the number of reactions that connect two species. Vertices are red for gas-phase species and blue for adsorbates.

the estimation of the activation barrier for the C–C cleavage in ethyl is based on work from Sutton et al.,[44] and is capable of predicting the activation barrier with reasonable accuracy, e.g. ±30 kJ mol^{-1}. Combining correlated uncertainties from the reaction enthalpy and the quasi-random perturbation in the slope and intercept leads to reasonable uncertainty distributions of the activation barrier. Overall, RMG can accurately estimate the energetic parameters and correlated uncertainty with the presented approach.

Since the mechanism generation is without bias within the constraint of the available reaction families, different energetic parameters will lead to different kinetically relevant pathways. This effect can be easily seen by tracking the metrics of the generated reaction mechanisms (see Figure 2c).

The number of kinetically relevant *core* species (gas+ surface) ranges from 25 to 44, with 50 to 177 important reactions. During the generation, RMG considers an additional 177 species, whose production rates never exceed the flux threshold and they remained in the *edge*, along with their 994 reactions. The total number of *core* and *edge* species/reactions depends on the user-defined tolerances

that decide which species and pathways are moved to the *core*, as well as the termination criterion. The correct selection of these values requires extensive testing, which was conducted in previous work for this system.[18] RMG requires around 2 minutes to generate a mechanism for this system, and the entire ensemble of 2000 mechanisms is constructed in approx. 100 CPU hours.

Within this ensemble of mechanisms, some species and reactions are discovered more often than others, which can highlight their importance in the uncertainty range, as illustrated in the reaction network in Figure 3d. The reaction mechanism consists to a large extent of abstraction reactions, including oxidative dehydrogenation (ODH) reactions and the abstraction of larger carbon-containing moieties. RMG now considers the formation and dissociation of bidentate adsorbates, which is a feature that has been added to the software recently. We truncated the mechanism exploration to adsorbates with two binding sites, due to the limited amount of thermophysical data and rate rules, but including multidentate adsorbates is possible. RMG applies the existing reaction templates to predict elementary steps for the bidentate adsorbates, exactly as it does for mono-
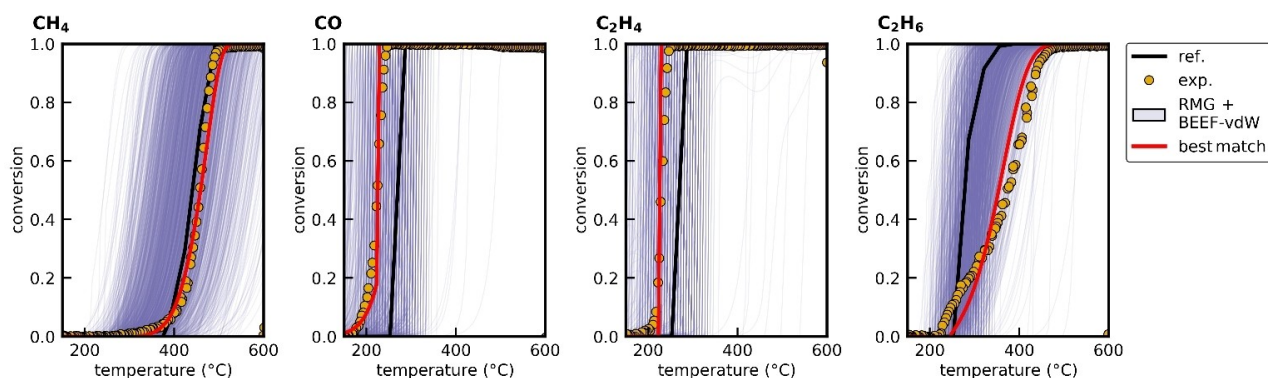
Figure 3. Comparison of conversion profiles from the light-out experiment with the microkinetic model predictions for CH_4, CO, C_2H_4, and C_2H_6. The blue area consists of the 2000 generated mechanisms from the BEEF-vdW ensemble and the black line is the reference mechanism with the unperturbed parameters. A single best-match microkinetic model (red line) can be identified that agrees remarkably well with the experimental data.

dentate species. This feature results in the discovery of many abstraction reactions involving bidentate adsorbates, which have been absent in most reported microkinetic models due to the combinatorial possibilities of reactions.[6,9] Additionally, bidentate adsorbates add to the microkinetic model's complexity and require approaches to deal with duplicate reactions (see SI) and resonance structures of adsorbates, well-known phenomena in the gas phase but hitherto not discussed in catalysis.

Figure 3 shows the microkinetic modeling results with the generated mechanisms using the open-source Cantera toolkit[45] and its plug-flow reactor code. Inter- and intra-particle mass transfer can be neglected due to the high volumetric flow rate and thin catalyst layer (see SI). Coverage effects for the self-interaction of *CO and *O were included in the mechanisms after the generation based on DFT calculations from previous work.[18] The experimentally recorded light-out curve shows the oxidation of CO and C_2H_4 at low temperatures, followed by C_2H_6 and CH_4. The reference mechanism is already in good agreement with the experimental results for CH_4, whereas the profiles for CO and C_2H_4 are slightly shifted to higher temperatures. In contrast, the onset for the conversion of C_2H_6 is at lower temperatures than in the experiment, and the profile's curvature does not match. Running the simulation with all generated microkinetic models within the correlated uncertainty reveals a broad band of possible solutions around the reference mechanism created with the default energetic parameters. Notably, deviations in the T_{50} of up to ± 150 K are observed for CH_4. These large deviations are mainly caused by parametric uncertainty of the microkinetic model and are not due to the structural uncertainty in the mechanism caused by the omission of pathways. All the pathways not included in the mechanisms by RMG are too slow, which is why their omission does not affect the conversion profiles. A previous study by Kreitz et al.[16] supports the hypothesis, where parameters of a single CO_2 methanation mechanism over Ni(111) were perturbed in their uncertainty space, which resulted in similar variations in the model predictions.

The predictions of the microkinetic model are densely clustered around the reference mechanism and sparsely populated towards the edges. The experimental profiles for CH_4, CO, and C_2H_4 are well within the center of the distribution. In contrast, C_2H_6 is shifted towards the edge of higher temperatures but still enclosed by the ensemble. Indeed, it is possible to identify a single reaction mechanism from this correlated uncertainty space of the Pt(111) facet that can simultaneously describe all the conversion profiles with excellent agreement. The microkinetic model in best agreement with the data is provided in the SI. There are small deviations at low temperatures for C_2H_6. However, we do not think that these discrepancies are caused by the omission of pathways but rather due to the simplified treatment of coverage effects, as well as the representation of a complex multifaceted catalyst with an extended Pt(111) surface. Including additional coverage effects for other adsorbates, cross interactions, and coverage-dependent activation barriers, can quantitatively change the results of the microkinetic model. Furthermore, experiments suggest dynamical changes of the catalyst such as oxidation[46] and re-dispersion[47,48] under operating conditions, which influence the available surface area, the distribution of facets, and ultimately the activity.

The relevant pathways for the emission oxidation are shown in Figure 4. It contains all the species that are discovered in each of the 2000 mechanisms (see Figure 2d). Additionally, all the energetic parameters of the important steps of the best match mechanism are based on BEEF-vdW calculations and not estimates. C_2H_4 adsorbs in a bidentate configuration and is dehydrogenated to form *CH*CH, which dissociates to form two *CH. Ethane adsorbs dissociatively to ethyl, which then forms di-σ bidentate ethylene. The rest of the pathway is similar to C_2H_4. The conversion of methane is also dominated by dissociation reactions that lead to *CH. Multiple pathways account for the conversion of *CH to *CO. *CH can either dissociate to form *C, which is oxidized to *CO, or it can form formyl (H*CO) via oxidation followed by the fission of the C–H bond. There is a small contribution from the reaction with

Figure 4. Reaction path diagram tracking the C element for the best match mechanism at a temperature of 400 °C and inlet conditions. The label on the arrows indicates the co-reactant. Pt represents a vacant surface site.

*OH to form carboxyl (O*COH), which produces CO_2 via an ODH reaction. In some of the generated mechanisms, side branches exist in the reaction network to convert ethylene and ethane via *CCH_3. This intermediate can be oxidized to CH_3*CO, followed by cleavage of the C–C bond to form *CH_3 and *CO. The described pathways are dominant along the length of the monolith and the entire temperature range (see Figure S11). Overall, the Pt-catalyzed oxidation of the hydrocarbons under stoichiometric conditions in the present study is dominated by a pyrolytic pathway to form *CH, which is then subsequently oxidized. The surface is most likely covered by *CO and *CH at low temperatures, followed by *O after *CO is oxidized (see Figure S12). Our findings differ from the work of Peela et al.,[49] who reported a significant contribution of ODH reactions and oxygenated C_2 intermediates for the oxidation of C_2H_6. However, they conducted their study under fuel-lean conditions, whereas the present work investigates stoichiometric combustion conditions.

Applying the degree of rate control (DRC) and sensitivity analyses for the kinetics and free energy of formation reveals broad variations in the rate-controlling steps and intermediates within the uncertainty range (see SI). We have previously reported on this behavior of the variability of the DRC.[16,17] Additionally, perturbing all the parameters within a large uncertainty space allows application of global sensitivity methods, such as polynomial chaos expansions, to derive total and joint sensitivity coefficients, but these techniques require a considerably larger number of samples due to the high dimensionality.[16,50]

Microkinetic models rarely demonstrate quantitative agreement with experiments, and a regression of the rate-controlling parameters is often required. We have shown this approach in a previous study and achieved an acceptable agreement with the experiment.[18] The presented approach is fundamentally different, as no individual parameters are regressed. Admittedly, varying all parameters a few hundred times can also be considered a simple fitting procedure. However, perturbing the parameters within their correlated uncertainty space obtained from the ensemble of energies from the BEEF-vdW functional means that we perturb the exchange-correlation functional, not the energetic parameters themselves. This perturbation in the exchange-correlation functional can be visualized by the ensemble of exchange enhancement factors F_x displayed in Figure 5. Therefore, it is possible to trace all the correlated uncertainty back to a unique exchange-correlation functional. The enhancement factor that results in the best match microkinetic model falls within the range of the common GGA functionals within the important range of the reduced density gradient for the surface chemistry ($s < 2$).[29] We do not want to overemphasize our findings of this best match

Figure 5. Ensemble of exchange enhancement factors F_x from the Bayesian error estimate of the BEEF-vdW functional as a function of the reduced density gradient s. Red is the enhancement factor corresponding to the mechanism in best agreement with the experiment. The upper dashed line is the Lieb-Oxford (LO) limit and the lower dashed line is the local density approximation (LDA) limit. The enhancement factors of other common GGA functionals are also displayed. The vertical line highlights the important range for adsorbates which is $s < 2$.

functional but rather highlight the fact that the constraints applied in the optimization can be explicitly mapped back to the exchange-correlation model. In principle, the method also allows tuning or selection of the DFT functional to produce optimal energetic parameters with a non-self-consistent calculation for a given system, which could be exploited in further electronic structure calculations. However, extrapolation of the results to other metals or even different Pt facets remains untested and may be limited since the best match functional compounds all remaining sources of uncertainty in the model (e.g. the dynamic catalyst morphology and the simplified treatment of coverage effects). Moreover, we note that self-consistent calculations may be challenging due to the non-monotonic increase in F_x, which could lead to numerical issues or induce density-based errors that lead to unphysical results. Overall, this approach produces a better result than our previous study by fitting the elementary steps with the highest DRC[18] (see Figure S15), and it is much faster.

In computational catalysis, it is common to search for the most efficient catalytic materials by exploiting simplistic scaling models and ML techniques. Researchers often assume a fixed mechanism in these studies and vary the kinetic parameters. This work highlights the large variability in the mechanism within a constrained uncertainty range. Although there is a common set of species, additional pathways can become relevant for some energetic parameter combinations. Linear scaling relations are integrated into RMG[15] and can be used to scale the thermophysical parameters. These scaling relations can be employed to generate microkinetic models for the entire descriptor space automatically. With the implementations in this work, it is now possible to also investigate the effect of correlated uncertainties at every point in the descriptor space. Walker and co-workers[24,25] demonstrated that BEEF-vdW overestimates the uncertainty in the energies, and the method can be improved by using better Bayesian statistics based on selected functionals.

In this study, we assumed that the catalyst could be described by using an extended Pt(111) slab. This assumption is rather simplistic, as real-world catalysts typically consist of nanoparticles with a certain particle size distribution where each particle has various exposed facets. Therefore, it is necessary to account for the multifaceted nature of the system to truly describe the experiments on an ab-initio basis.[51] RMG can generate mechanisms for all possible Pt facets of a multifaceted crystal, if energetic databases are available and the structural uncertainty could, thus, be integrated in the correlated uncertainty quantification. Still, the method discussed in the present study allows us to determine whether the assumed facet could potentially be the active site if the predictions of the generated microkinetics enclose the experiment. Otherwise, there is a mismatch in the active site motif that causes the discrepancy such as e.g. different active facet(s) or the omission of metal/support interactions. Nonetheless, within the uncertainty of the parameter space and the simplifications in the microkinetic model, it is possible to find a set of parameters that can accurately describe the recorded experimental profiles.

This agreement can indicate that the Pt(111) facet is the active site or dominates the activity to a large extent. However, it is impossible to become more certain, even with additional DFT calculations since the parameters of the *core* mechanism are based on BEEF-vdW energies. That is why it will be necessary to decrease the uncertainty in the electronic structure method by using higher levels of theory, such as Quantum Monte Carlo methods[52] and exploiting error cancellation techniques.[53] Overall, the presented methodology is an extremely powerful tool to efficiently perform an exhaustive mechanism exploration and help gather the most influential elementary steps and intermediates, whose energetic parameters can be refined by higher-level of theory electronic structure calculations.

Conclusion

This study presents the first automated mechanism generation study considering correlated uncertainties from the BEEF-vdW functional in all energetic parameters. Every generated mechanism and microkinetic model can be traced back to an individual exchange-correlation functional. The method presented herein highlights the significant changes in the mechanism when perturbing the parameters in their uncertainty range, as demonstrated for the oxidation reactions of exhaust gas emissions over Pt(111). It was possible to identify a mechanism within the ensemble of candidates that reproduces experimental results with excellent accuracy. In addition to the exhaustive mechanism construction in the uncertainty range, the framework can also provide a tool for an ab-initio based parameter optimization approach to generate microkinetics in agreement with experiments. This generic framework is a fast method for constructing first-principles-based microkinetic models and is universally applicable to other heterogeneously catalyzed systems, including different facets, metals, and heteroatoms.

Conflict of Interest

The authors declare no conflict of interest.

Data Availability Statement

The data that support the findings of this study are openly available in zenodo at 10.5281/zenodo.7916529, reference number [33].

[1] G. D. Wehinger, M. Ambrosetti, R. Cheula, Z.-B. Ding, M. Isoz, B. Kreitz, K. Kuhlmann, M. Kutscherauer, K. Niyogi, J. Poissonnier, R. Réocreux, D. Rudolf, J. Wagner, R. Zimmermann, M. Bracconi, H. Freund, U. Krewer, M. Maestri, *Chem. Eng. Res. Des.* **2022**, *184*, 39–58.

[2] A. Bruix, J. T. Margraf, M. Andersen, K. Reuter, *Nat. Catal.* **2019**, *2*, 659–670.

[3] I. A. W. Filot, R. A. van Santen, E. J. M. Hensen, *Angew. Chem. Int. Ed.* **2014**, *53*, 12746–12750.

[4] B. W. J. Chen, L. Xu, M. Mavrikakis, *Chem. Rev.* **2021**, *121*, 1007–1048.

[5] L. Chanussot, A. Das, S. Goyal, T. Lavril, M. Shuaibi, M. Riviere, K. Tran, J. Heras-Domingo, C. Ho, W. Hu, A. Palizhati, A. Sriram, B. Wood, J. Yoon, D. Parikh, C. L. Zitnick, Z. Ulissi, *ACS Catal.* **2021**, *11*, 6059–6072.

[6] J. T. Margraf, K. Reuter, *ACS Omega* **2019**, *4*, 3370–3379.

[7] Q. Zhao, Y. Xu, J. Greeley, B. M. Savoie, *Nat. Commun.* **2022**, *13*, 4860.

[8] V. Streibel, H. A. Aljama, A.-C. Yang, T. S. Choksi, R. S. Sánchez-Carrera, A. Schäfer, Y. Li, M. Cargnello, F. Abild-Pedersen, *ACS Catal.* **2022**, *12*, 1742–1757.

[9] G. H. Gu, M. Lee, Y. Jung, D. G. Vlachos, *Nat. Commun.* **2022**, *13*, 2087.

[10] C. W. Gao, J. W. Allen, W. H. Green, R. H. West, *Comput. Phys. Commun.* **2016**, *203*, 212–225.

[11] M. Liu, A. Grinberg Dana, M. S. Johnson, M. J. Goldman, A. Jocher, A. M. Payne, C. A. Grambow, K. Han, N. W. Yee, E. J. Mazeau, K. Blondal, R. H. West, C. F. Goldsmith, W. H. Green, *J. Chem. Inf. Model.* **2021**, *61*, 2686–2696.

[12] G. Pio, X. Dong, E. Salzano, W. H. Green, *Combust. Flame* **2022**, *241*, 112080.

[13] F. H. Vermeire, S. U. Aravindakshan, A. Jocher, M. Liu, T.-C. Chu, R. E. Hawtof, R. Van de Vijver, M. B. Prendergast, K. M. Van Geem, W. H. Green, *Energy Fuels* **2022**, *36*, 1304–1315.

[14] K. Blondal, J. Jelic, E. Mazeau, F. Studt, R. H. West, C. F. Goldsmith, *Ind. Eng. Chem. Res.* **2019**, *58*, 17682–17691.

[15] E. J. Mazeau, P. Satpute, K. Blöndal, C. F. Goldsmith, R. H. West, *ACS Catal.* **2021**, *11*, 7114–7125.

[16] B. Kreitz, K. Sargsyan, K. Blöndal, E. J. Mazeau, R. H. West, G. D. Wehinger, T. Turek, C. F. Goldsmith, *JACS Au* **2021**, *1*, 1656–1673.

[17] B. Kreitz, G. D. Wehinger, C. F. Goldsmith, T. Turek, *ChemCatChem* **2022**, *14*, e202200570.

[18] B. Kreitz, P. Lott, J. Bae, K. Blöndal, S. Angeli, Z. W. Ulissi, F. Studt, C. F. Goldsmith, O. Deutschmann, *ACS Catal.* **2022**, *12*, 11137–11151.

[19] J. E. Sutton, W. Guo, M. A. Katsoulakis, D. G. Vlachos, *Nat. Chem.* **2016**, *8*, 331–337.

[20] A. J. Medford, J. Wellendorff, A. Vojvodic, F. Studt, F. Abild-Pedersen, K. W. Jacobsen, T. Bligaard, J. K. Nørskov, *Science* **2014**, *345*, 197–200.

[21] T. Gu, B. Wang, S. Chen, B. Yang, *ACS Catal.* **2020**, *10*, 6346–6355.

[22] Y. Lu, B. Wang, S. Chen, B. Yang, *J. Mol. Catal.* **2022**, *530*, 112575.

[23] G. R. Wittreich, G. H. Gu, D. J. Robinson, M. A. Katsoulakis, D. G. Vlachos, *J. Phys. Chem. C* **2021**, *125*, 18187–18196.

[24] E. A. Walker, D. Mitchell, G. A. Terejanu, A. Heyden, *ACS Catal.* **2018**, *8*, 3990–3998.

[25] E. Walker, S. C. Ammal, G. A. Terejanu, A. Heyden, *J. Phys. Chem. C* **2016**, *120*, 10328–10339.

[26] C. Fricke, B. Rajbanshi, E. A. Walker, G. Terejanu, A. Heyden, *ACS Catal.* **2022**, *12*, 2487–2498.

[27] Z. Ulissi, V. Prasad, D. G. Vlachos, *J. Catal.* **2011**, *281*, 339–344.

[28] B. Wang, S. Chen, J. Zhang, S. Li, B. Yang, *J. Phys. Chem. C* **2019**, *123*, 30389–30397.

[29] J. Wellendorff, K. T. Lundgaard, A. Møgelhøj, V. Petzold, D. D. Landis, J. K. Nørskov, T. Bligaard, K. W. Jacobsen, *Phys. Rev. B* **2012**, *85*, 235149.

[30] X. Shi, R. Seiser, J.-Y. Chen, R. Dibble, R. Cattolica, *SAE Int. J. Engines* **2015**, *8*, 1246–1252.

[31] C. F. Goldsmith, R. H. West, *J. Phys. Chem. C* **2017**, *121*, 9970–9981.

[32] W. H. Green, R. H. West, "RMG—Reaction Mechanism Generator," can be found under https://rmg.mit.edu/**2023** (accessed 30.01.2023).

[33] "Data for Automated Generation of Microkinetics for Heterogeneously Catalyzed Reactions Considering Correlated Uncertainties": B. Kreitz, P. Lott, A. J. Medford, F. Studt, O. Deutschmann, Goldsmith, C. Franklin, zenodo **2023**, https://doi.org/10.5281/zenodo.791.

[34] M. S. Johnson, X. Dong, A. Grinberg Dana, Y. Chung, D. Farina, R. J. Gillis, M. Liu, N. W. Yee, K. Blondal, E. Mazeau, C. A. Grambow, A. M. Payne, K. A. Spiekermann, H.-W. Pang, C. F. Goldsmith, R. H. West, W. H. Green, *J. Chem. Inf. Model.* **2022**, *62*, 4906–4915.

[35] R. G. Susnow, A. M. Dean, W. H. Green, P. Peczak, L. J. Broadbelt, *J. Phys. Chem. A* **1997**, *101*, 3731–3740.

[36] J. Wellendorff, T. L. Silbaugh, D. Garcia-Pintos, J. K. Nørskov, T. Bligaard, F. Studt, C. T. Campbell, *Surf. Sci.* **2015**, *640*, 36–44.

[37] F. Studt, *Front. Catal.* **2021**, *1*, 658965.

[38] T. Avanesian, S. Dai, M. J. Kale, G. W. Graham, X. Pan, P. Christopher, *J. Am. Chem. Soc.* **2017**, *139*, 4551–4558.

[39] B. Ruscic, R. E. Pinzon, G. von Laszewski, D. Kodeboyina, A. Burcat, D. Leahy, D. Montoy, A. F. Wagner, *J. Phys. Conf. Ser.* **2005**, *16*, 561–570.

[40] C. F. Goldsmith, *Top. Catal.* **2012**, *55*, 366–375.

[41] E. D. Hermes, K. Sargsyan, H. N. Najm, J. Zádor, *J. Chem. Theory Comput.* **2019**, *15*, 6536–6549.

[42] E. Araujo-Lopez, B. D. Vandegehuchte, D. Curulla-Ferré, D. I. Sharapa, F. Studt, *J. Phys. Chem. C* **2020**, *124*, 27503–27510.

[43] A. Gremminger, J. Pihl, M. Casapu, J.-D. Grunwaldt, T. J. Toops, O. Deutschmann, *Appl. Catal. B* **2020**, *265*, 118571.

[44] J. E. Sutton, D. G. Vlachos, *Ind. Eng. Chem. Res.* **2015**, *54*, 4213–4225.

[45] D. G. Goodwin, R. L. Speth, H. K. Moffat, B. W. Weber, "Cantera: An Object-Oriented Software Toolkit for Chemical Kinetics, Thermodynamics, and Transport Processes," can be found under https://www.cantera.org**2023** (accessed 30.01.2023).

[46] F. Maurer, A. Gänzler, P. Lott, B. Betz, M. Votsmeier, S. Loridant, P. Vernoux, V. Murzin, B. Bornmann, R. Frahm, O.

Deutschmann, M. Casapu, J.-D. Grunwaldt, *Ind. Eng. Chem. Res.* **2021**, *60*, 6662–6675.

[47] A. M. Gänzler, M. Casapu, D. E. Doronkin, F. Maurer, P. Lott, P. Glatzel, M. Votsmeier, O. Deutschmann, J.-D. Grunwaldt, *J. Phys. Chem. Lett.* **2019**, *10*, 7698–7705.

[48] A. M. Gänzler, M. Casapu, P. Vernoux, S. Loridant, F. J. Cadete Santos Aires, T. Epicier, B. Betz, R. Hoyer, J.-D. Grunwaldt, *Angew. Chem. Int. Ed.* **2017**, *56*, 13078–13082.

[49] N. R. Peela, J. E. Sutton, I. C. Lee, D. G. Vlachos, *Ind. Eng. Chem. Res.* **2014**, *53*, 10051–10058.

[50] H. Tian, S. Rangarajan, *ACS Catal.* **2020**, *10*, 13535–13542.

[51] B. Kreitz, G. D. Wehinger, C. F. Goldsmith, T. Turek, *J. Phys. Chem. C* **2021**, *125*, 2984–3000.

[52] G. R. Iyer, B. M. Rubenstein, *J. Phys. Chem. A* **2022**, *126*, 4636–4646.

[53] B. Kreitz, K. Abeywardane, C. F. Goldsmith, *J. Chem. Theory Comput.* **2023**, *19*, 4149–4162.
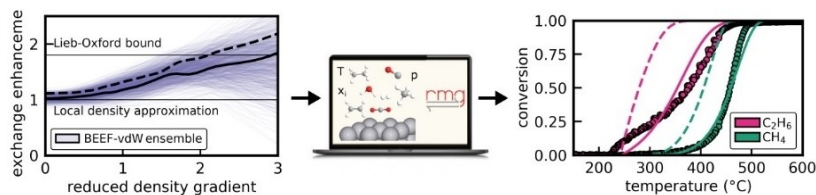
Research Articles

Reaction Networks

B. Kreitz,* P. Lott, F. Studt, A. J. Medford,
O. Deutschmann,
C. F. Goldsmith* ———— e202306514

Automated Generation of Microkinetics for Heterogeneously Catalyzed Reactions Considering Correlated Uncertainties

The Reaction Mechanism Generator (RMG) is used to automatically generate an ensemble of mechanisms for the oxidation of emissions over Pt(111). By sampling energetic parameters from the uncertainty space of the BEEF-vdW functional, every generated mechanism corresponds to a different DFT functional. From the broad range of predictions, it is possible to identify microkinetic models that achieve remarkable agreement with experiments.